ORIGINAL RESEARCH

Prevalence of Plateau Iris in Primary Angle Closure Glaucoma: An Egyptian Hospital Based Ultrasound Biomicroscopy Study

Amira E Hamad[1], Ahmed F Elmaria [2], Tarek R Hussein[2], Said M Shalaby[2]

[1]Tanta Ophthalmology Hospital, Ministry of Health, Tanta, Elgharbia Province, Egypt; [2]Department of Ophthalmology, Tanta University, Tanta, Elgharbia Province, Egypt

Correspondence: Ahmed F Elmaria, Department of Ophthalmology, Tanta University, Tanta, Elgharbia Province, 31527, Egypt, Tel +20 1020306017, Email ahmed.fekry@med.tanta.edu.eg

Purpose: To determine the distribution and the anatomical characteristics of plateau iris (PI) in primary angle closure glaucoma (PACG) using ultrasound biomicroscopy (UBM).

Methods: Fifty UBM images of PACG cases were studied over one year by retrospective analysis. The data from UBM images including angle opening distance at 500 and 750 μm (AOD500 and AOD750), trabecular-iris angle (TIA), angle recess area at 750 μm (ARA750), maximum ciliary body thickness (CBTmax), anterior placement of ciliary processes (APCP), central anterior chamber depth (CACD), axial lens thickness (ALT), and ciliary sulcus status were analyzed and compared between the PI and non-PI cases.

Results: Eighteen cases had PI (36%). The mean AOD500, AOD750, and TIA were significantly smaller in PI than in non-PI eyes ($P = 0.01$; $P = 0.046$; and $P = 0.026$). Values of the ARA750 and CBTmax were not significantly different between the two groups ($P = 0.208$ and $P = 0.368$). CACD was deeper in the PI group ($P = 0.011$). ALT was higher in the non-PI group ($P = 0.001$). The mean APCP of the PI group was more than those of the non-PI group ($P < 0.001$). The number of cases with obliterated ciliary sulcus in more than two quadrants was significantly more in the PI group ($P < 0.001$).

Conclusion: Around one-third of PACG eyes were found to have PI on UBM imaging. The number of obliterated ciliary sulcus and APCP were important UBM parameters that help in PI diagnosis.

Keywords: UBM, plateau iris, primary angle closure glaucoma

Introduction

Primary angle closure glaucoma (PACG) is one of the major causes of blindness globally; however, if detected early enough, permanent damage to the optic nerve and trabecular meshwork can be avoided. Population-based researches demonstrate that PACG has a three-fold greater risk of severe, bilateral vision impairment when compared to the rates of blindness in primary open angle glaucoma.[1,2]

There are many mechanisms of PACG such as relative pupillary block, crystalline lens thickness and position, and plateau iris (PI). In Chinese patients, around half of the PACG was produced by mixed mechanisms, one-third (38.1%) was caused by pure relative pupillary block, and less than 10% (7.1%) was caused by pure non-pupillary block mechanisms.[3]

PI is one of the most frequent causes of PACG in young adult patients.[4] In PI, the ciliary processes are anteriorly rotated and sustain the convexity of the peripheral iris, thus closing the ciliary sulcus and causing trabecular iris contact (TIC).[5] He et al described three PI variants in the Chinese eye. Typical PI has an anteriorly rotated ciliary body that pushes the peripheral iris. The second variant has a thick peripheral iris that angulates abruptly to insert into the middle of the ciliary body front surface. The third variant has only a bulky peripheral iris.[6]

Clinically, PI is suspected in eyes with normal central anterior chamber depth (CACD) but shallow at the periphery. Diagnosis can be confirmed by the "double hump" sign on indentation gonioscopy in eyes with angle closure.[7]

Ultrasound biomicroscopy (UBM) provides in vivo imaging of the anterior segment of the eye and is a very useful tool in glaucoma in general and PACG in special as it can clearly outline the anatomy of structures sharing in anterior chamber angle crowding and tailor the management of every case by directing the treatment to the most contributing factor causing PACG.[8–10]

Kumar et al described the UBM image of the PI by the anteriorly rotated ciliary body, obliterated ciliary sulcus, steep iris root from its point of insertion followed by a downward angulation, flat iris plane, and TIC.[11]

This study aimed to determine the proportion of PI among cases of PACG in a tertiary eye hospital in Elgharbia, Egypt, and to examine different quantitative and qualitative UBM parameters of the PI and non-PI iris mechanisms for PACG.

Materials and Methods
Materials
This study represents a retrospective analysis of the recorded UBM images of 50 cases diagnosed with PACG who attended Tanta University Eye Hospital over one year from January 2019 to December 2019. The study was reviewed and approved by the Ethical Committee of the Faculty of Medicine, Tanta University (approval code: 33927/7/20) and adhered to the tenets of the Declaration of Helsinki. Informed consent was waived due to the retrospective nature of the study. Subjects' privacy and confidentiality were preserved through coding of the data.

Inclusion Criteria
1. Patients diagnosed with PACG (≥180 degrees TIC with peripheral anterior synechia, elevated intraocular pressure, and optic neuropathy).[12]
2. Both genders were included in the study.

Exclusion Criteria
1. Eyes with a secondary cause of angle closure such as (neovascular, uveitic, traumatic, and malignant glaucoma).
2. Patients with a history of intraocular surgery, penetrating eye trauma, and any anterior segment abnormalities that might affect the results.

Study Groups
Based on the UBM images, subjects were divided into two groups, PI, and non-PI. Kumar UBM-based criteria were used to diagnose PI, which had to be met in at least two quadrants.[11]

Methods
UBM Imaging Acquisition
The examination was performed using Vu-Max™ UBM device (Sonomed, Inc., New York, USA) with a 35 MHz transducer probe. All patients were previously examined in a supine position in a semi-dark room. The reviewed images for every case were sulcus-to-sulcus axial scan passing through the center of the pupil and four radial scans at the 12, 6, 3, and 9 clock positions centered over the limbus.

UBM Obtained Parameters
1. Angle Opening Distance at 500 and 750 μm (AOD500, AOD750): The distance from the point 500 and 750 μm anterior to the scleral spur to the iris surface along a line drawn perpendicular to the corneal-scleral inner surface.[13]
2. Trabecular Iris Angle 500 μm (TIA500): The apex of the angle in the iris recess and the arms passing through a point on the trabecular meshwork 500 μm from the scleral spur and the other point on the iris perpendicularly.[14]
3. Angle Recess Area 750 μm (ARA750): The enclosed triangular area is demarcated by the anterior iris surface, trabecular meshwork, and corneal endothelium out to 750 μm from the scleral spur.[15]
4. Maximum Ciliary Body Thickness (CBTmax): The distance from the most inner point of the ciliary processes to the inner wall of the sclera or its extended line.[16]
5. Anterior Placement of Ciliary Processes (APCP): The distance from the most anterior point of the ciliary body to the perpendicular line from the inner wall of the sclera passing through the scleral spur.[16]
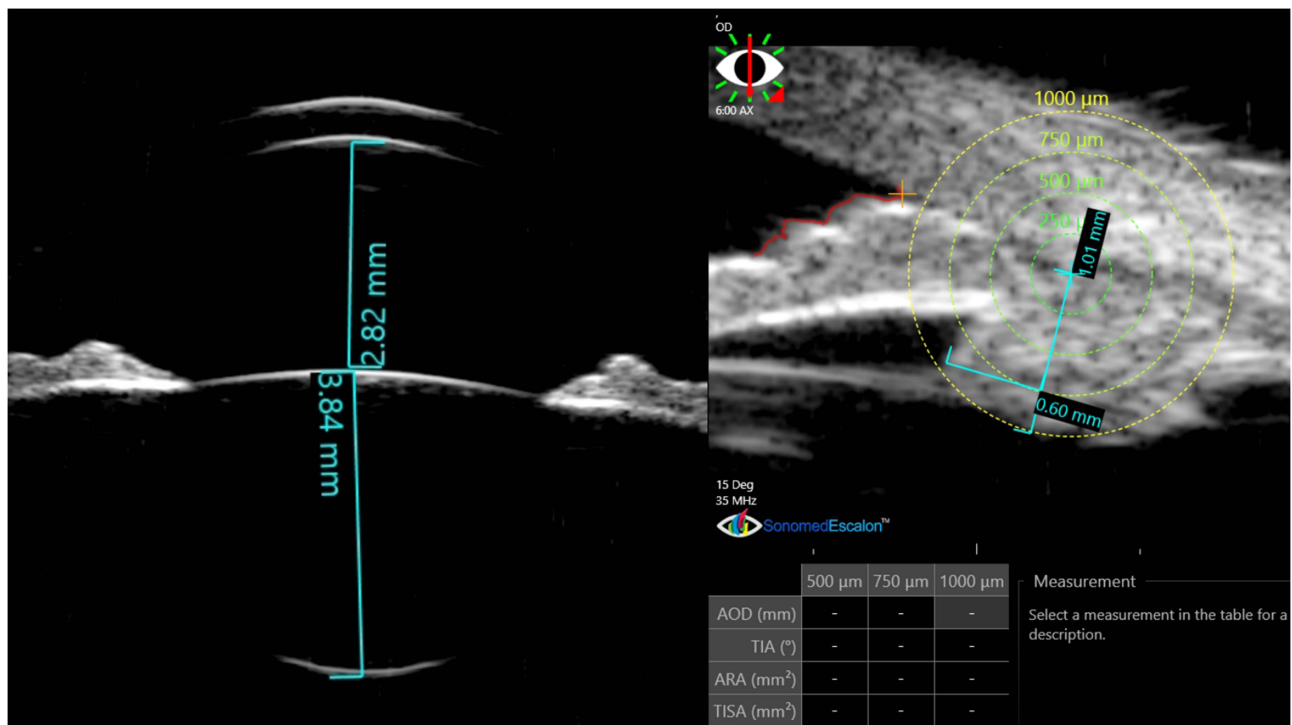
Figure 1 UBM image of one case, sulcus-to-sulcus axial scan (left), and lower quadrant radial scan (right), both are labeled with the measured parameters.

6. Central Anterior Chamber Depth (CACD): The distance from the central corneal endothelial surface to the center of the anterior lens capsule, measured from the image of sulcus-to-sulcus axial scan passing through the center of the cornea and the pupil.[17]
7. Axial Lens Thickness (ALT): The distance from the anterior pole to the posterior pole of the lens.
8. Ciliary Sulcus: The space between the posterior surface of the iris base and the anterior surface of the ciliary body and noted as present or obliterated.

Figure 1 shows two recorded images (axial and lower radial scans) of one case. After manually locating the position of the scleral spur, the included UBM software package automatically detected AOD, TIA, and ARA parameters, while other quantitative data were measured manually using the software metering tool.

Statistical Analysis

Data analysis was performed using IBM SPSS Statistics for Windows, Version 20.0. Armonk, NY: IBM Corp. Quantitative data were described using mean and standard deviation, and qualitative data were described using numbers and percentages. To compare the two groups: the Student's t-test was used for normally distributed quantitative data, and the Mann Whitney test was employed for abnormally distributed quantitative variables. Chi-square test was used to compare the categorical variables. For each UBM parameter, a receiver operating characteristic (ROC) curve was generated, and the area under the curve (AUC) was calculated to identify the most independent factors for the UBM diagnosis of PI. P-value 0.05 was chosen as the significance level.

Results

Demographic Data

There were 18 out of 50 studied PACG cases diagnosed with PI according to UBM images (36.0%). Table 1 shows no significant differences between the PI and non-PI groups regarding gender distribution ($P = 0.75$) and age ($P = 0.14$).

Table I Demographic Characteristics (the Age and Gender Distribution) of the Study Groups

	Plateau Iris (n = 18)	Non-Plateau Iris (n = 32)	P[a]
Sex [n (%)]			
Male	7 (38.9)	11 (34.4)	0.750
Female	11 (61.1)	21 (65.6)	
Age (years)			
Mean ± SD.	52.78 ± 9.11	56.88 ± 9.48	0.143

Note: [a]Student's *t*-test of significance for continuous variables and Chi-square test for categorical variables between the two groups.
Abbreviation: SD, standard deviation.

Comparative Analysis of Data from UBM Images of the PI and Non-PI Groups

Table 2 indicates that four quadrants and average AOD500 and AOD750 of the PI group were significantly smaller than those of the non-PI group. The TIA in the four quadrants did not differ statistically between the two groups, but the average TIA was significantly lower in the PI group (*P* = 0.026). The 4 quadrants and average ARA750 and CBTmax were not significantly different between both groups. The 4 quadrants and average APCP of the PI group showed significantly more anterior position than those of the non-PI group. The mean CACD was significantly deeper in the PI group (*P* = 0.011). ALT was significantly more in the non-PI group (*P* = 0.001). The number of eyes with obliterated ciliary sulcus in more than two quadrants was significantly more in the PI group (*P* < 0.001). Figure 2 shows UBM images of an eye with a PI mechanism, and Figure 3 shows a PACG eye with non-PI.

UBM Parameters' Ability to Discriminate Between PI and Non-PI Groups

ROC curve was constructed for each UBM parameter for detecting PI (Figures 4 and 5). Table 3 represents the predictive measures of each UBM parameter to classify subjects into the PI and non-PI groups. The number of obliterated ciliary sulcus quadrants was an outstanding test with the area under the curve (AUC = 0.969), APCP was an excellent test (AUC = 0.814), while other UBM parameters were acceptable to fair tests.

Discussion

In this study, 18 cases (36%) were diagnosed with PI out of 50 studied UBM images for subjects with PACG. Mochizuki et al[18] found Plateau iris configurations (PIC) in 34.6% of patients with PACG. Mansoori et al[19] showed PIC in 83/262 PACG eyes with a percentage of 31.68%. Kumar et al[20] noted that PIC was present in 28.7% of the cases with PACG.

The quadrant-wise analysis in the present study showed that PI was more prevalent in the superior and inferior quadrants followed by nasal and temporal quadrants. Kumar et al[20] showed that the superior quadrant was the most involved, followed by inferior, nasal, and temporal quadrants. Mizoguchi et al[21] found that the prevalence of PIC is more in the nasal quadrant followed by superior, then temporal, and then inferior quadrant; this may be explained by different ethnicity (Asian population).

The results of our study comparing different UBM parameters between the PI and non-PI groups showed that the mean average of AOD500 and AOD750 were significantly smaller in the PI group (*P* = 0.01, *P* = 0.04, respectively). Shabana et al[17] found that the means of AOD500 and AOD750 in the PIC were statistically significant differences between PI and other mechanisms of PACG (*P* = 0.04, *P* < 0.001, respectively). Moghimi et al[22] showed non-significant difference regarding AOD500 and AOD750 between PI and pupillary block mechanisms (*P* = 0.53, *P* = 0.98 respectively).

The average TIA of the PI group was significantly less than that of the non-PI group (*P* = 0.026). We did not find a significant difference between the PI and non-PI groups regarding ARA750 and CBTmax. To our knowledge, no published data comparing these three UBM parameters between PI and other mechanisms of PACG.

Table 2 Comparative Analysis of Data from UBM Images of the 2 Study Groups

	Plateau Iris (n = 18)	Non-Plateau Iris (n = 32)	P^a
AOD 500 (Mean ± SD)			
12 O'clock	0.01 ± 0.02	0.03 ± 0.05	0.002*
3 O'clock	0.06 ± 0.11	0.08 ± 0.10	0.022*
6 O'clock	0.01 ± 0.03	0.04 ± 0.06	0.008*
9 O'clock	0.09 ± 0.11	0.12 ± 0.09	0.049*
Average	0.04 ± 0.08	0.06 ± 0.08	0.01*
AOD 750 (Mean ± SD)			
12 O'clock	0.06 ± 0.08	0.09 ± 0.09	0.024*
3 O'clock	0.11 ± 0.15	0.14 ± 0.14	0.049*
6 O'clock	0.06 ± 0.08	0.11 ± 0.15	0.018*
9 O'clock	0.13 ± 0.16	0.22 ± 0.09	0.005*
Average	0.09 ± 0.09	0.14 ± 0.08	0.046*
TIA 500 (Mean ± SD)			
12 O'clock	2.75 ± 11.67	6.43 ± 13.08	0.168
3 O'clock	8.05 ± 14.36	22.67 ± 25.69	0.054
6 O'clock	4.86 ± 14.13	10.47 ± 20.68	0.220
9 O'clock	21.35 ± 24.99	20.47 ± 24.65	0.789
Average	9.25 ± 18.2	15 ± 22.4	0.026*
ARA 750 (Mean ± SD)			
12 O'clock	0.01 ± 0.02	0.01 ± 0.02	0.566
3 O'clock	0.03 ± 0.05	0.05 ± 0.07	0.378
6 O'clock	0.01 ± 0.01	0.02 ± 0.03	0.571
9 O'clock	0.04 ± 0.05	0.05 ± 0.07	0.624
Average	0.02 ± 0.04	0.03 ± 0.05	0.208
CBTmax (Mean ± SD)			
12 O'clock	1.22 ± 0.14	1.21 ± 0.18	0.882
3 O'clock	1.30 ± 0.18	1.21 ± 0.17	0.089
6 O'clock	0.15 ± 1.23	0.16 ± 1.16	0.435
9 O'clock	1.22 ± 0.15	1.18 ± 0.15	0.340
Average	1.24 ± 0.15	± 0.16	0.368
APCB (Mean ± SD)			
12 O'clock	0.70 ± 0.23	0.41 ± 0.24	<0.001*
3 O'clock	0.73 ± 0.30	0.47 ± 0.28	0.002*
6 O'clock	0.82 ± 0.39	0.54 ± 0.20	0.015*
9 O'clock	0.77 ± 0.30	0.50 ± 0.28	0.004*
Average	0.75 ± 0.30	0.47 ± 0.25	<0.001*
CACD (Mean ± SD)	2.44 ± 0.26	2.15 ± 0.43	0.011*
ALT (Mean ± SD)	4.04 ± 0.26	4.35 ± 0.29	0.001*
Ciliary Sulcus [n (%)]			
12 O'clock			<0.001*
Obliterated	15 (83.3)	7 (21.9)	
Present	3 (16.7)	25 (78.1)	
3 O'clock			0.006*
Obliterated	11 (61.1)	7 (21.9)	
Present	7 (38.9)	25 (78.1)	
6 O'clock			0.001*
Obliterated	15 (83.3)	11 (34.4)	
Present	3 (16.7)	21 (65.6)	
9 O'clock			0.001*
Obliterated	11 (61.1)	5 (15.6)	
Present	7 (38.9)	27 (74.4)	
Obliterated in ≥2 quadrants	18 (100)	6 (18.75)	<0.001*

**Notes**: [a]Mann Whitney test of significance for continuous variables and Chi-square test for categorical variables between the two groups; *Statistically significant at $P \leq 0.05$.
Abbreviations: AOD, angle opening distance; TIA, trabecular iris angle; ARA, angle recession area; CBTmax, maximum ciliary body thickness; APCP, anterior placement of ciliary processes; CACD, central anterior chamber depth; ALT, axial length thickness.
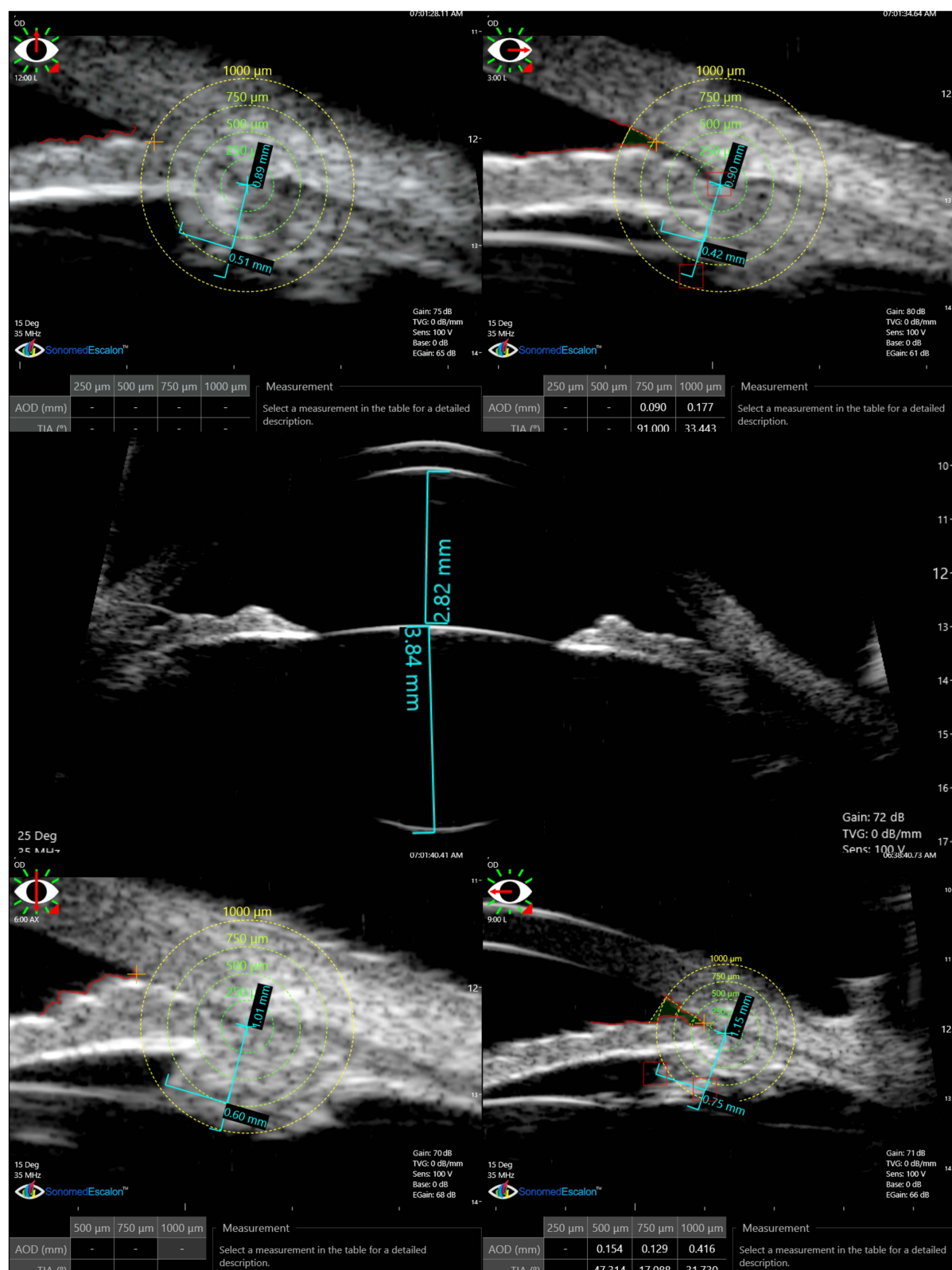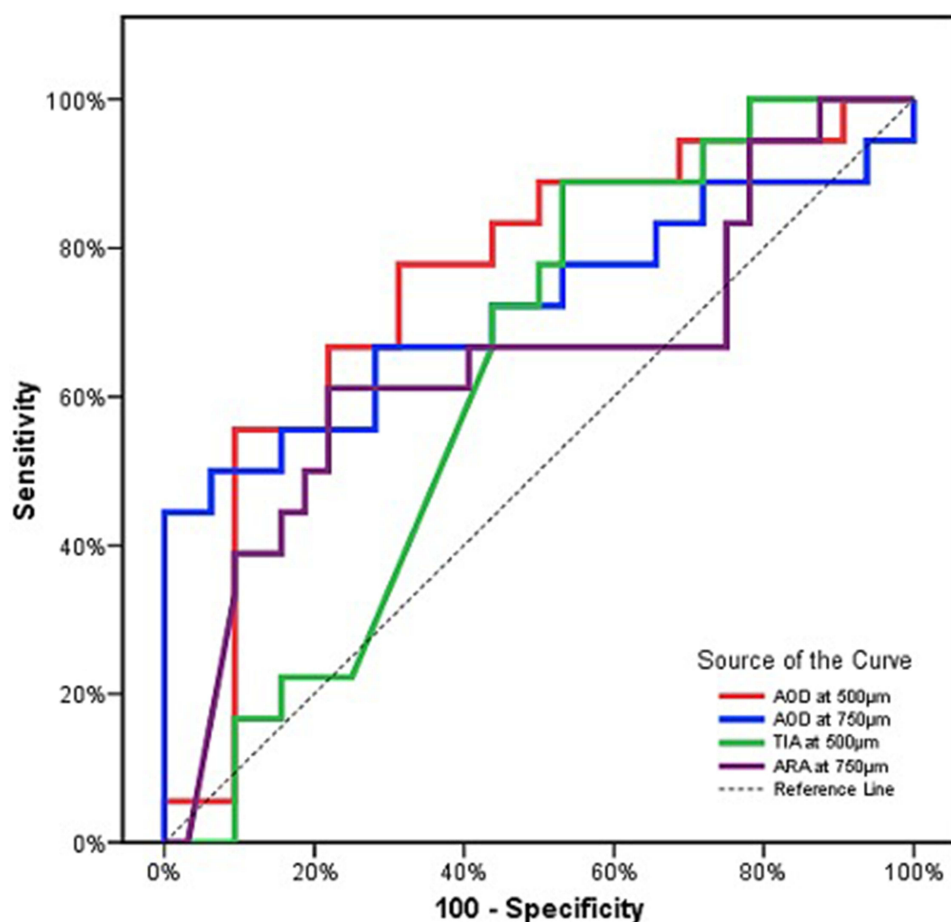
Figure 2 Collage of images of sulcus-to-sulcus axial scan and 4 quadrant scans at 12, 3, 6, and 9 clock hours of a case in the PI group.
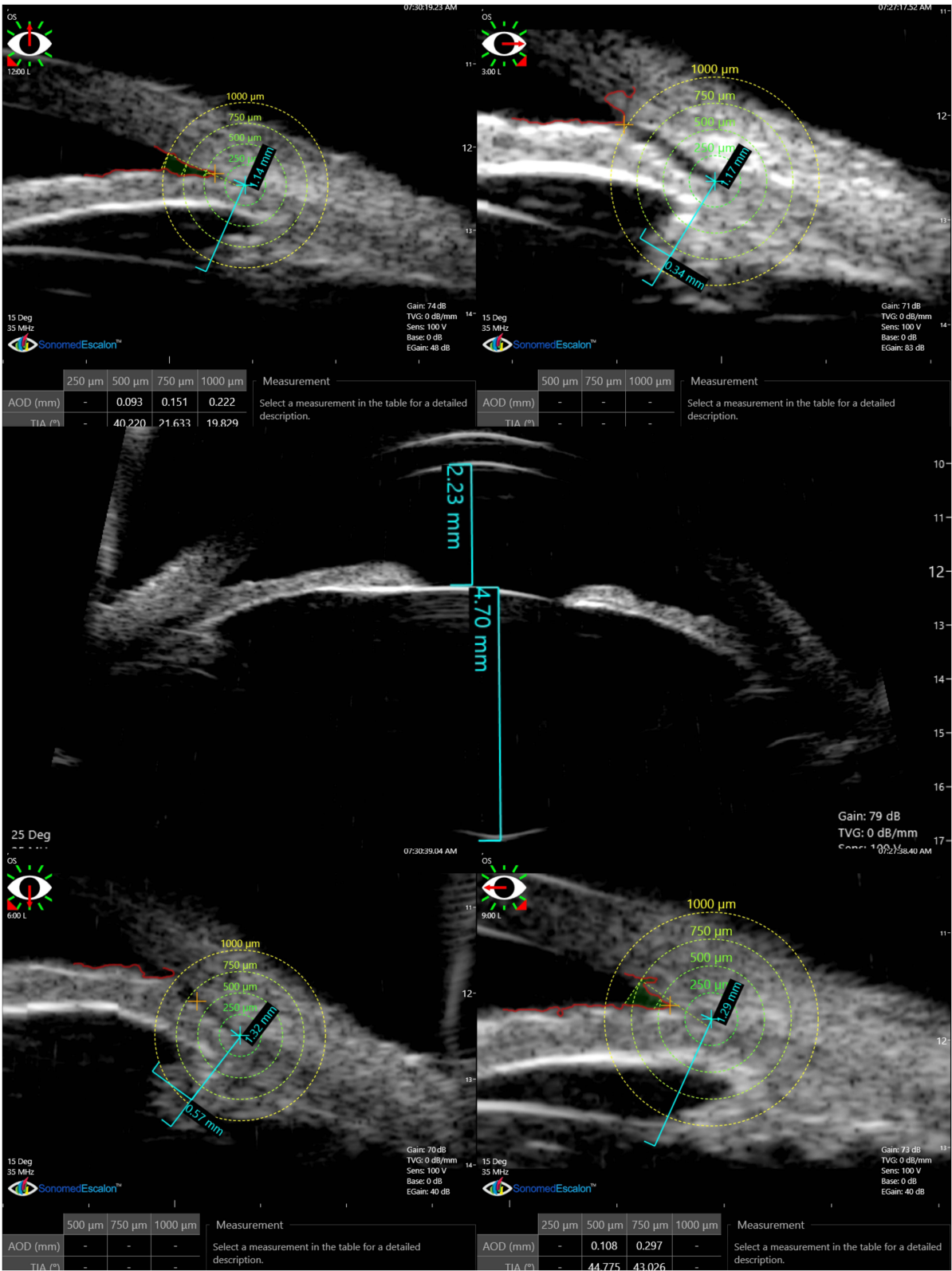
Figure 3 Collage of images of sulcus-to-sulcus axial scan and 4 quadrant scans at 12, 3, 6, and 9 clock hours of a case in the non-PI group.

Figure 4 ROC curves for AOD 500, AOD 750, TIA 500, and ARA 750 UBM parameters to discriminate PI from non-PI.

The current results showed that the mean of average APCP is significantly higher in PI than in non-PI ($P < 0.001$). Garudadri et al[23] detected more anteriorly placed ciliary processes with narrow ciliary sulcus in 22 of 33 eyes (66.66%) with PACG in the Indian patients even after laser peripheral iridotomy.

The mean CACD was significantly higher in the PI group ($P = 0.011$). This result agrees with many UBM and anterior segment optical coherence tomography studies.[7,17,24] Moghimi et al[22] does not support our result as they found a non-significant CACD difference between PI and pupillary block mechanisms of PACG ($P = 0.12$).

The crystalline lens was significantly thicker in the non-PI group ($P = 0.001$). Chen et al[24] used A-scan ultrasonography to compare the ocular characteristics among PI, pupillary block, and normal eyes and found a significant lens thickness difference between PI and pupillary block ($P < 0.001$). Contrary to these results, Mizoguchi et al[21] found that there was a non-significant difference in the mean value of ALT between PI and non-PI groups ($P = 0.15$), which may be due to different ethnic patients, Japanese subjects, involved in their study.

Numbers of obliterated ciliary sulcus quadrants have statistically significant differences in the mean value between the PI and non-PI groups ($P < 0.001$).

Among the tested UBM parameters, the AUC was highest in the number of obliterated ciliary sulcus quadrants followed by APCP.

There are certain limitations to our study. The small sample size and the fact that participants with PACG were recruited from a single institution; might have caused bias.
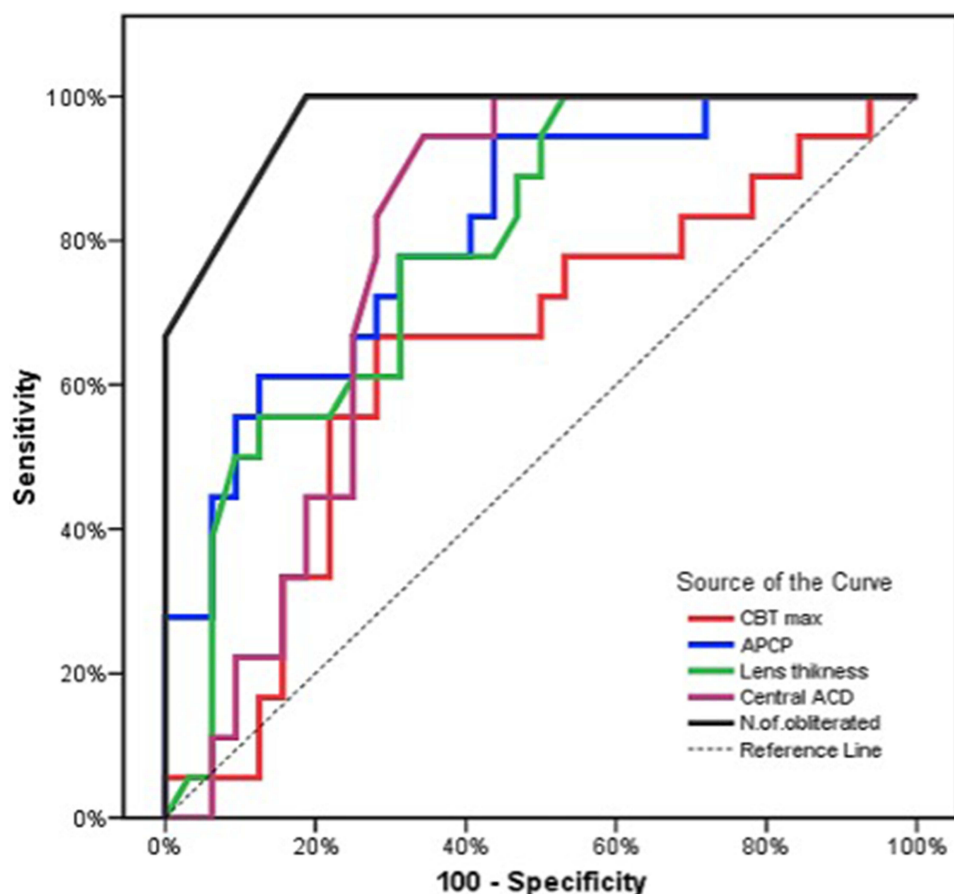
Figure 5 ROC curves for CBT max, APCP, lens thickness, central ACD, and the number of obliterated ciliary sulcus UBM parameters to discriminate PI from non-PI.

Conclusion

We found a thirty-six percent of subjects with PACG have PI in a tertiary eye hospital in Elgharbia, Egypt, based on specific UBM criteria. Ophthalmologists need to consider this aspect while managing patients with PACG, as the response to treatment may differ depending on the mechanism involved. UBM image data aid in the PI diagnosis, especially the number of quadrants with obliterated ciliary sulcus and APCP.

Table 3 Predictive Measures of UBM Parameters for PI and Non-PI Classification

UBM Parameter	AUC	Sensitivity %	Specificity %	PPV %	NPV %	Accuracy %
AOD at 500μm	0.750	55.56	84.38	66.67	77.14	74.0
AOD at 750μm	0.719	50.0	93.75	81.82	76.92	78.0
TIA at 500μm	0.628	11.11	90.63	40.0	64.44	62.0
ARA at 750μm	0.648	0.0	100.0	–	64.0	64.0
CBTmax	0.642	16.67	87.50	42.86	65.12	62.0
APCP	0.814	55.56	90.63	76.92	78.38	78.0
CACD	0.785	38.89	81.25	53.85	70.27	66.0
ALT	0.790	50.0	90.63	75.0	76.32	76.0
Number of obliterated Ciliary Sulcus quadrants	0.969	100.0	81.25	75.0	100.0	88.0

Abbreviations: AOD, angle opening distance; TIA, trabecular iris angle; ARA, angle recession area; CBTmax, maximum ciliary body thickness; APCP, anterior placement of ciliary processes; CACD, central anterior chamber depth; ALT, axial length thickness; AUC, area under the curve.

Disclosure

The authors report no conflicts of interest in this work.

References

1. Tham Y-C, Li X, Wong TY, Quigley HA, Aung T, Cheng C-Y. Global prevalence of glaucoma and projections of glaucoma burden through 2040: a systematic review and meta-analysis. *Ophthalmology*. 2014;121:2081–2090. doi:10.1016/j.ophtha.2014.05.013
2. Sun X, Dai Y, Chen Y, et al. Primary angle closure glaucoma: what we know and what we don't know. *Prog Retin Eye Res*. 2017;57:26–45. doi:10.1016/j.preteyeres.2016.12.003
3. Wang N, Ouyang J, Zhou W, et al. Multiple patterns of angle closure mechanisms in primary angle closure glaucoma in Chinese. *Zhonghua Yan Ke Za Zhi Chin J Ophthalmol*. 2000;36:46–51.
4. Stefan C, Iliescu DA, Batras M, Timaru CM, De Simone A. Plateau iris–diagnosis and treatment. *Roman J Ophthalmol*. 2015;59:14.
5. Pavlin CJ, Ritch R, Foster FS. Ultrasound biomicroscopy in plateau iris syndrome. *Am J Ophthalmol*. 1992;113:390–395. doi:10.1016/S0002-9394(14)76160-4
6. He M, Foster PJ, Johnson GJ, Khaw PT. Angle-closure glaucoma in East Asian and European people. Different diseases? *Eye*. 2006;20:3–12. doi:10.1038/sj.eye.6701797
7. Kiuchi Y, Kanamoto T, Nakamura T. Double hump sign in indentation gonioscopy is correlated with presence of plateau iris configuration regardless of patent iridotomy. *J Glaucoma*. 2009;18:161–164. doi:10.1097/IJG.0b013e31817d23b5
8. Dada T, Gadia R, Sharma A, et al. Ultrasound biomicroscopy in glaucoma. *Surv Ophthalmol*. 2011;56:433–450. doi:10.1016/j.survophthal.2011.04.004
9. El Salhy AA, Elseht RM, Al Maria AF, Shalaby SW, Hossein TR. Functional evaluation of the filtering bleb by ultrasound biomicroscopy after trabeculectomy with mitomycin C. *Int J Ophthalmol*. 2018;11:245–250. doi:10.18240/ijo.2018.02.11
10. Mannino G, Abdolrahimzadeh B, Calafiore S, Anselmi G, Mannino C, Lambiase A. A review of the role of ultrasound biomicroscopy in glaucoma associated with rare diseases of the anterior segment. *Clin Ophthalmol*. 2016;10:1453–1459. doi:10.2147/OPTH.S112166
11. Kumar RS, Tantisevi V, Wong MH, et al. Plateau Iris in Asian subjects with primary angle closure glaucoma. *Arch Ophthalmol*. 2009;127:1269–1272. doi:10.1001/archophthalmol.2009.241
12. Prum BEJ, Herndon LWJ, Moroi SE, et al. Primary angle closure preferred practice pattern(®) guidelines. *Ophthalmology*. 2016;123:P1–40. doi:10.1016/j.ophtha.2015.10.049
13. Moghimi S, Vahedian Z, Fakhraie G, et al. Ocular biometry in the subtypes of angle closure: an anterior segment optical coherence tomography study. *Am J Ophthalmol*. 2013;155:664–673, 673.e1. doi:10.1016/j.ajo.2012.10.014
14. Henzan IM, Tomidokoro A, Uejo C, et al. Ultrasound biomicroscopic configurations of the anterior ocular segment in a population-based study the Kumejima study. *Ophthalmology*. 2010;117:1720–1728, 1728.e1. doi:10.1016/j.ophtha.2010.01.045
15. Pavlin CJ, Harasiewicz K, Foster FS. Ultrasound biomicroscopy of anterior segment structures in normal and glaucomatous eyes. *Am J Ophthalmol*. 1992;113:381–389. doi:10.1016/S0002-9394(14)76159-8
16. Wang Z, Huang J, Lin J, Liang X, Cai X, Ge J. Quantitative measurements of the ciliary body in eyes with malignant glaucoma after trabeculectomy using ultrasound biomicroscopy. *Ophthalmology*. 2014;121:862–869. doi:10.1016/j.ophtha.2013.10.035
17. Shabana N, Aquino MCD, See J, et al. Quantitative evaluation of anterior chamber parameters using anterior segment optical coherence tomography in primary angle closure mechanisms. *Clin Experiment Ophthalmol*. 2012;40:792–801. doi:10.1111/j.1442-9071.2012.02805.x
18. Mochizuki H, Takenaka J, Sugimoto Y, Takamatsu M, Kiuchi Y. Comparison of the prevalence of plateau iris configurations between angle-closure glaucoma and open-angle glaucoma using ultrasound biomicroscopy. *J Glaucoma*. 2011;20:315–318. doi:10.1097/IJG.0b013e3181e3d2da
19. Mansoori T, Sarvepally VK, Balakrishna N. Plateau iris in primary angle closure glaucoma: an ultrasound biomicroscopy study. *J Glaucoma*. 2016;25:e82–86. doi:10.1097/IJG.0000000000000263
20. Kumar G, Bali SJ, Panda A, Sobti A, Dada T. Prevalence of plateau iris configuration in primary angle closure glaucoma using ultrasound biomicroscopy in the Indian population. *Indian J Ophthalmol*. 2012;60:175–178. doi:10.4103/0301-4738.95865
21. Mizoguchi T, Ozaki M, Wakiyama H, Ogino N. Plateau iris in Japanese patients with primary angle closure and primary angle closure glaucoma. *Clin Ophthalmol*. 2015;9:1159–1163. doi:10.2147/OPTH.S80724
22. Moghimi S, Kiaroudi M, Coh P, Li Y, He M, Lin SC. Comparison of anterior chamber parameters in patients with plateau iris configuration and pupillary block using ASOCT. *J Glaucoma*. 2017;26:153–158. doi:10.1097/IJG.0000000000000579
23. Garudadri CS, Chelerkar V, Nutheti R. An ultrasound biomicroscopic study of the anterior segment in Indian eyes with primary angle-closure glaucoma. *J Glaucoma*. 2002;11:502–507. doi:10.1097/00061198-200212000-00009
24. Chen YY, Chu D, Chou P. Enhancing the early differential diagnosis of plateau iris and pupillary block using a-scan ultrasonography. *PLoS One*. 2015;10:e0118811. doi:10.1371/journal.pone.0118811